

Gas-Phase Structure of 4-(4-hydroxyphenylazo)phthalonitrile - Precursor for Synthesis of Phthalocyanines with Macrocyclic and Azo Chromophores

Alexander E. Pogonin[@], Ivan Yu. Kurochkin, Alexander V. Krasnov, Alyona S. Malyasova, Ilya A. Kuzmin, Tatyana V. Tikhomirova and Georgiy V. Girichev

Ivanovo State University of Chemistry and Technology, Ivanovo, 153000, Russian Federation

[@]Corresponding author E-mail: pogonin@isuct.ru, pogoninalexander@mail.ru

Table S1. Conditions of GED experiments for <i>p</i> -HPhAPN.....	2
Table S2. The most intensive ions in the mass spectrum of <i>p</i> -HPhAPN were recorded by APDM-1 during the combined GED/MS experiment.	2
Figure S1. Comparison of theoretical radial distribution functions <i>f</i> (<i>r</i>) of different structures of <i>p</i> -HPhAPN.....	3
Table S3. Z-matrix used for model <i>c</i> in the GED refinement.	4
Table S4. Z-matrix used for model <i>a</i> in the GED refinement.....	5
Table S5. Z-matrix used for model <i>e</i> in the GED refinement.....	6
Table S6. Z-matrix was used for model <i>f</i> in the GED refinement.	7
Table S7. Nucleus-independent chemical shifts (NICS) ^a indexes for <i>E-AB</i> and <i>p</i> -HPhAPN.....	8
Table S8. Electron delocalization indexes (DI) calculated by QTAIM for several structures of <i>p</i> -HPhAPN.....	8
Figure S2. Calculated (GFN2-xTB) EI-MS (below, inverted intensities) of <i>E-AB</i> in comparison with the experimental EI-MS [75] (above).....	9
Figure S3. Comparison of EI-MS obtained using the QCxMS (GFN2-xTB) procedures started separately for <i>E-AB</i> (above) and <i>Z-AB</i> (below, inverted intensities) structures.....	9
Figure S4. Comparison of EI-MS of <i>p</i> -HPhAPN obtained using the QCxMS (GFN2-xTB) procedures started separately for <i>a</i> (above) and <i>za</i> (below, inverted intensities) structures.....	10
Figure S5. Comparison of calculated (GFN2-xTB) EI-MS of <i>p</i> -HPhAPN isomers <i>a</i> (above) and <i>e</i> (below, inverted intensities).	10
Figure S6. Temperature dependence of conformational/isomeric composition of <i>p</i> -HPhAPN.....	11
Figure S7. Experimental (cycles) and theoretical (red solid lines) radial distribution curve for models <i>c</i> and <i>a</i> of <i>p</i> -HPhAPN and the difference curve $\Delta f(r)$ (blue solid line).....	12
Figure S8. Experimental (cycles) and theoretical (red solid lines) radial distribution curve for models <i>f</i> and <i>e</i> of <i>p</i> -HPhAPN and the difference curve $\Delta f(r)$ (blue solid line).	13
Table S9. Semi-experimental parameters of <i>p</i> -HPhAPN (azo forms <i>a</i> and <i>c</i>).	14
Table S10. Relative energies ^a of different isomers of <i>Zn-tHPhDaPc</i> obtained using different forms (<i>a</i> , <i>c</i> , <i>e</i> , <i>f</i>) of <i>p</i> -HPhAPN.	17
Table S11. Internuclear distances (\AA) ^a of zinc complex <i>Zn-tHPhDaPc</i> obtained using <i>a</i> and <i>c</i> forms of <i>p</i> -HPhAPN and corresponding Internuclear distances of <i>p</i> -HPhAPN (models <i>a</i> and <i>c</i>).	17
Table S12. Nucleus-independent chemical shifts (NICS) ^a indexes for Zinc phtalocyanine (ZnPc) and <i>Zn-tHPhDaPc</i>	18

Table S1. Conditions of GED experiments for *p-HPhAPN*.

L, mm	338	598
N	4	4
I, μA	1.73	1.00
λ , \AA	0.04272(4)	0.04158(4)
T, K	464(5)	463(5)
t, s	68	60
p_{col} , Torr	$2 \cdot 10^{-6}$	$2.1 \cdot 10^{-6}$
p_{MS} , Torr	$6.0 \cdot 10^{-7}$	$6.0 \cdot 10^{-7}$
$S_{\text{min}}\text{-}S_{\text{max}}(\Delta s)$, \AA^{-1}	2.3-27.6 (0.1)	1.3-16.2 (0.1)
U_{ion} , V	50	50

L - distance from nozzle to plate; N - number of recorded films; I - primary electron beam current; λ - electron wavelength; T - effusion cell temperature; t - exposure time; p_{col} - residual gas pressure in diffraction chamber, p_{MS} - residual gas pressure in mass spectrometry unit; $S_{\text{min}}\text{-}S_{\text{max}}(\Delta s)$, range and step (in brackets) of scattering angles; U_{ion} - ionization voltage.

Table S2. The most intensive ions in the mass spectrum of *p-HPhAPN* were recorded by APDM-1 during the combined GED/MS experiment.

m/z	Relative intensity, %	
	Experiment with L=338 mm	Experiment with L=598 mm
248	25	24
127	12	11
121	38	37
100	8	6
93	100	100
65	53	52
52	9	9

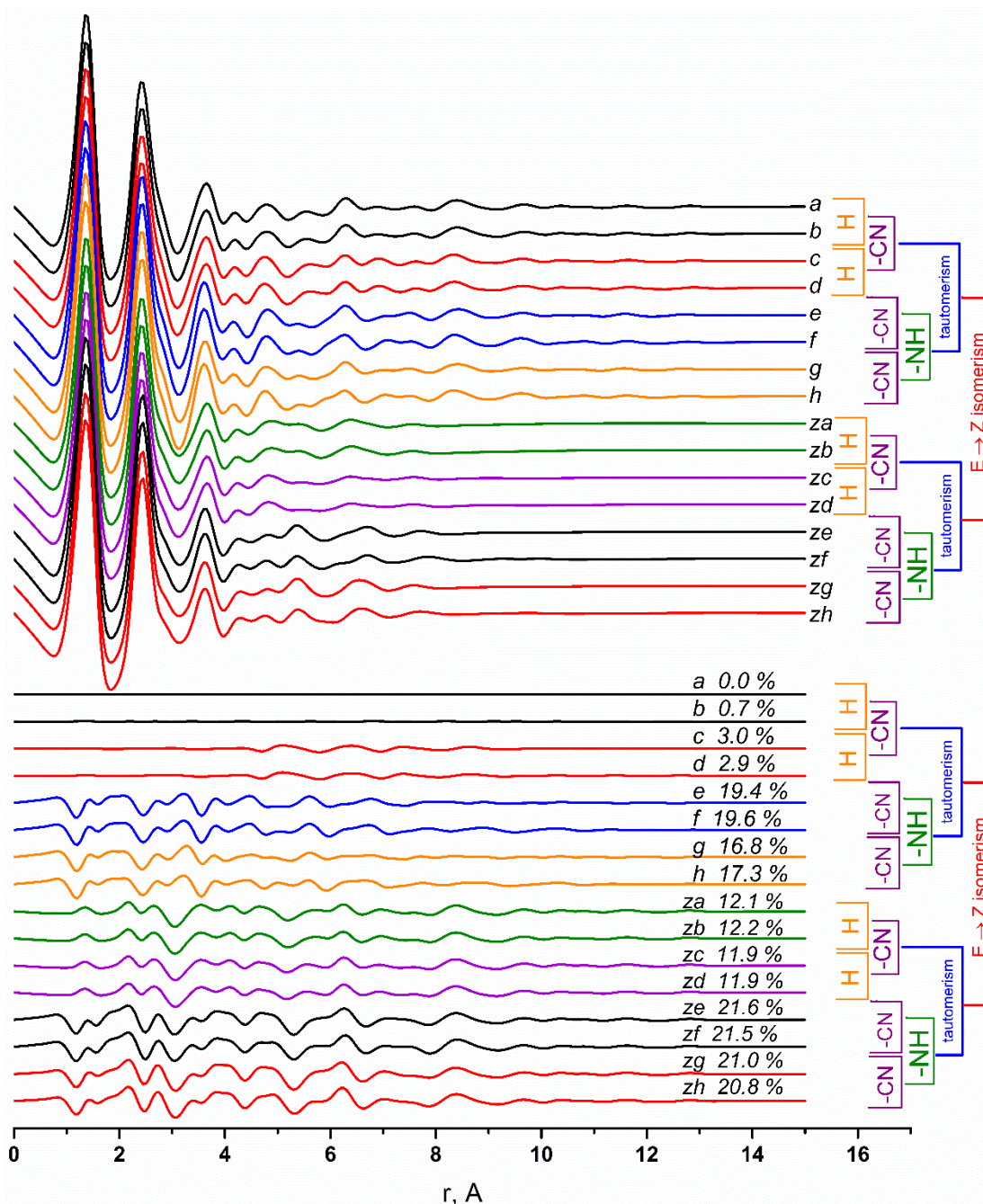


Figure S1. Comparison of theoretical radial distribution functions $f(r)$ of different structures of ***p*-HPHAPN**.

Differences functions $\Delta f(r)$ were calculated concerning model **a**. Differences between the models (a possible path of transition from structure to structure) are presented to the right of the picture: “H” - different arrangement of hydrogen atoms of the hydroxyl group (rotation of the hydroxyl group around the CO bond or rotation of the -Ph-OH group around the N'1-C'2 bond); “-CN” – cisoid/transoid arrangement of nitrile groups concerning the azo/hydrazone group (rotation of the -Ph-2CN moiety around the N1-C2 bond); “tautomerism” – enol and keto forms; “-NH” – the presence of a bond between a H and N1/N'1 atoms; “E-→Z- isomerism” – trans- and cis- isomers.

Vibrational amplitudes and vibrational corrections ($r_{h1}-r_a$) to nuclear distances were calculated on the base of force field obtained from QC calculations using VibModule program for the temperature $T = 450$ K. Calculations of the model radial distributions curves $f(r)$ were performed in the UNEX programming environment. The difference curves $\Delta f(r)$ were calculated relative to the curve corresponding to structure **a** (Figure 3): $\Delta f(r) = f_j(r) - f_a(r)$. The deviation of the j -th curve from the reference curve was characterized by disagreement factor ($R_{f,j}$) between the theoretical molecular scattering intensities corresponding to different models:

$$R_{f,j} = \sqrt{\frac{\sum_{i=1}^N (sM(s_i)_a - k_M sM(s_i)_{\text{model } j})^2}{\sum_{i=1}^N (sM(s_i)_{\text{model } j})^2}} \cdot 100\%$$

where $sM(s_i)_a$ is theoretical molecular scattering intensities for structure **a**; $sM(s_i)_{\text{model } j}$ – theoretical molecular scattering intensities for the corresponding model (Figure 3); k_M – is the scale.

Table S3. Z-matrix used for model *c* in the GED refinement.

Body of Z-matrix					
1 N					
2 N 1 NN					
3 C 1 RN1 2 AN1					
4 C 2 RN1_1 AN1_3 T					
5 C 3 RCC1 1 AC1 2 T1					
6 C 4 RCC1_2 AC1_1 T1_					
7 C 5 RCC2 3 AC2 1 T2					
8 C 6 RCC2_4 AC2_2 T2_					
9 C 7 RCC3 5 AC3 3 TPh1					
10 C 8 RCC3_6 AC3_4 TPh1_					
11 C 9 RCC4 7 AC4 5 TPh2					
12 C 10 RCC4_8 AC4_6 TPh2_					
13 C 3 RCC5 11 RCC6 5 TPh3 4					
14 C 4 RCC5_12 RCC6_6 TPh3_ 4					
15 C 7 R_CCN1 9 A_CCN1 5 T_CCN1					
16 C 9 R_CCN2 7 A_CCN2 11 T_CCN2					
17 N 15 RNC1 7 A_NC1 9 T_NC1					
18 N 16 RNC2 9 A_NC2 11 T_NC2					
19 O 10 RCO 8 ACO 12 TCO					
20 H 5 RCH1 3 ACH1 7 TH1					
21 H 6 RCH1_4 ACH1_8 TH1_					
22 H 8 RCH2_6 ACH2_10 TH2					
23 H 11 RCH3 9 ACH3 13 TH3					
24 H 12 RCH3_10 ACH3_14 TH3_					
25 H 13 RCH4 3 ACH4 11 TH4					
26 H 14 RCH4_4 ACH4_12 TH4_					
27 H 19 ROH 10 AOH 12 TOH					
Variables Values		Atom numbering			
NN	1.252312022647	1	A_CCN1	121.005200500574	40
RN1	1.413565101242	2	A_CCN2	121.193321723491	41
RN1_	1.400441863466	3	A_NC1	178.827324171675	42
RCC1	1.392796278330	4	A_NC2	178.577197349465	43
RCC1_	1.405728244799	5	ACO	116.933579920227	35
RCC2	1.392930900148	6	ACH1	119.026268136813	46
RCC2_	1.376639021061	7	ACH1_	119.169904982746	47
RCC3	1.408749240029	8	ACH2_	121.381012059742	49
RCC3_	1.401033345283	9	ACH3	118.890942065064	50
RCC4	1.400466654366	10	ACH3_	120.078720312775	51
RCC4_	1.394899063397	11	ACH4	119.168401260387	52
RCC5	1.401034940728	12	ACH4_	118.546915191703	53
RCC6	1.380491350003	14	AOH	110.598209348084	45
RCC5_	1.397342017381	13	T	180.000000000000	54
RCC6_	1.383944146724	15	T1	180.000000000000	55
R_CCN1	1.428898779228	16	T1_	0.000000000000	56
R_CCN2	1.426393784777	17	T2	180.000000000000	57
RNC1	1.151185488734	18	T2_	180.000000000000	58
RNC2	1.151769557883	19	TPh1	0.000000000000	59
RCO	1.356051937467	20	TPh1_	0.000000000000	60
RCH1	1.080019624274	22	TPh2	0.000000000000	61
RCH1_	1.079463986613	23	TPh2_	0.000000853774	62
RCH2_	1.080676067579	25	TPh3	180.000000000000	63
RCH3	1.080481209337	26	TPh3_	180.000000000000	64
RCH3_	1.082885185848	27	T_CCN1	180.000000000000	65
RCH4	1.079087525841	28	T_CCN2	180.000000000000	66
RCH4_	1.080972098001	29	T_NC1	180.000000000000	67
ROH	0.961908859459	21	T_NC2	0.000000000000	68
AN1	114.788608110929	30	TCO	180.000000000000	69
AN1_	116.278040268057	31	TH1	180.000000000000	71
AC1	115.363270520380	32	TH1_	180.000000000000	72
AC1_	124.939894077781	33	TH2	180.000000000000	73
AC2	120.604749041739	34	TH3	180.000000000000	75
AC2_	120.185924092671	34	TH3_	180.000000000000	76
AC3	119.613805422335	34	TH4	180.000000000000	77
AC3_	119.998003844527	34	TH4_	180.000000000000	78
AC4	119.275063234531	34	TOH	0.000000000000	70
AC4_	120.286540382266	34			

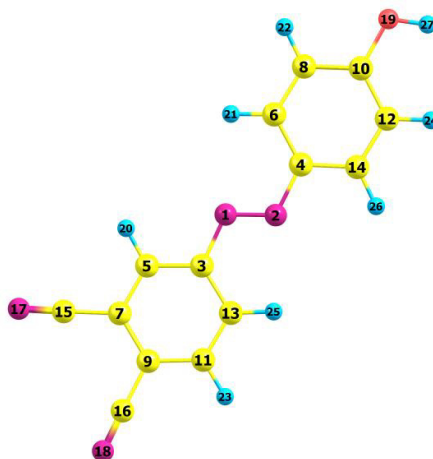


Table S4. Z-matrix used for model **a** in the GED refinement.

Body of Z-matrix			
1	N		
2	N	1	NN
3	C	1 RN1 2	AN1
4	C	2 RN1_ 1 AN1_ 3	T
5	C	3 RCC1 1 AC1 2	T1
6	C	4 RCC1_ 2 AC1_ 1	T1_
7	C	5 RCC2 3 AC2 1	T2
8	C	6 RCC2_ 4 AC2_ 2	T2_
9	C	7 RCC3 5 AC3 3	TPh1
10	C	8 RCC3_ 6 AC3_ 4	TPh1_
11	C	9 RCC4 7 AC4 5	TPh2
12	C	10 RCC4_ 8 AC4_ 6	TPh2_
13	C	3 RCC5 11 RCC6 5	TPh3 4
14	C	4 RCC5_ 12 RCC6_ 6	TPh3_ 4
15	C	7 R_CCN1 9 A_CCN1 5	T_CCN1
16	C	9 R_CCN2 7 A_CCN2 11	T_CCN2
17	N	15 RNC1 7 A_NC1 9	T_NC1
18	N	16 RNC2 9 A_NC2 11	T_NC2
19	O	10 RCO 8 ACO 12	TCO
20	H	5 RCH1 3 ACH1 7	TH1
21	H	6 RCH1_ 4 ACH1_ 8	TH1_
22	H	8 RCH2_ 6 ACH2_ 10	TH2
23	H	11 RCH3 9 ACH3 13	TH3
24	H	12 RCH3_ 10 ACH3_ 14	TH3_
25	H	13 RCH4 3 ACH4 11	TH4
26	H	14 RCH4_ 4 ACH4_ 12	TH4_
27	H	19 ROH 10 AOH 12	TOH

Variables Values				Atom numbering	
NN	1.252304959926	1	A_CCN1	120.708473509361	40
RN1	1.413960081334	2	A_CCN2	121.097206065438	41
RN1_	1.399822304022	3	A_NC1	178.752800487518	42
RCC1	1.397747261860	4	A_NC2	178.655294344919	43
RCC1_	1.405702960860	5	ACO	116.925889112794	35
RCC2	1.389022152965	6	ACH1	119.566817720645	46
RCC2_	1.376621190572	7	ACH1_	119.165348895908	47
RCC3	1.413466128441	8	ACH2_	121.397565715783	49
RCC3_	1.401117837997	9	ACH3	119.211346985680	50
RCC4	1.395858430685	10	ACH3_	120.087136525558	51
RCC4_	1.394873863059	11	ACH4	118.570047801755	52
RCC5	1.395660825944	12	ACH4_	118.542935183960	53
RCC6	1.384277078697	14	AOH	110.587695833867	45
RCC5_	1.397490359290	13	T	180.000000000000	54
RCC6_	1.383847458525	15	T1	0.000000000000	255
R_CCN1	1.429846801274	16	T1_	0.000001207418	56
R_CCN2	1.426513837110	17	T2	180.000000000000	57
RNC1	1.151166172566	18	T2_	180.000000000000	58
RNC2	1.151753675794	19	TPh1	0.000000000000	59
RCO	1.356035357582	20	TPh1_	0.000000000000	60
RCH1	1.078732946561	22	TPh2	0.000000000000	61
RCH1_	1.079475763045	23	TPh2_	0.000000000000	62
RCH2_	1.080685667845	25	TPh3	180.000000000000	63
RCH3	1.080078677664	26	TPh3_	179.999999146226	64
RCH3_	1.082868620067	27	T_CCN1	180.000000000000	65
RCH4	1.080630685681	28	T_CCN2	180.000000000000	66
RCH4_	1.080959607410	29	T_NC1	180.000000000000	67
ROH	0.961936695864	21	T_NC2	0.000000000000	68
AN1	114.783064703585	30	TCO	180.000000000000	69
AN1_	116.411601781376	31	TH1	180.000000000000	71
AC1	124.431804874377	232	TH1_	180.000000000000	72
AC1_	124.972037012343	33	TH2	180.000000000000	73
AC2	120.080451700319	34	TH3	180.000000000000	75
AC2_	120.179450827777	34	TH3_	180.000000000000	76
AC3	120.109185829077	34	TH4	180.000000000000	77
AC3_	119.991072885450	34	TH4_	180.000000000000	78
AC4	119.245259497158	34	TOH	0.000000853774	70
AC4_	120.296229298867	34			

Table S5. Z-matrix used for model *e* in the GED refinement.

Body of Z-matrix			
1 N			
2 N 1 NN			
3 C 1 RN1 2 AN1			
4 C 2 RN1_1 AN1_3 T			
5 C 3 RCC1 1 AC1 2 T1			
6 C 4 RCC1_2 AC1_1 T1_			
7 C 5 RCC2 3 AC2 1 T2			
8 C 6 RCC2_4 AC2_2 T2_			
9 C 7 RCC3 5 AC3 3 TPh1			
10 C 8 RCC3_6 AC3_4 TPh1_			
11 C 9 RCC4 7 AC4 5 TPh2			
12 C 10 RCC4_8 AC4_6 TPh2_			
13 C 3 RCC5 11 RCC6 5 TPh3 4			
14 C 4 RCC5_12 RCC6_6 TPh3_ 4			
15 C 7 R_CCN1 9 A_CCN1 5 T_CCN1			
16 C 9 R_CCN2 7 A_CCN2 11 T_CCN2			
17 N 15 RNC1 7 A_NC1 9 T_NC1			
18 N 16 RNC2 9 A_NC2 11 T_NC2			
19 O 10 RCO 8 ACO 12 TCO			
20 H 5 RCH1 3 ACH1 7 TH1			
21 H 6 RCH1_4 ACH1_8 TH1_			
22 H 8 RCH2_6 ACH2_10 TH2			
23 H 11 RCH3 9 ACH3 13 TH3			
24 H 12 RCH3_10 ACH3_14 TH3_			
25 H 13 RCH4 3 ACH4 11 TH4			
26 H 14 RCH4_4 ACH4_12 TH4_			
27 H 1 RNH 2 ANH 4 TNH			
Variables Values		Atom numbering	
NN	1.323347737775	301	A_CCN1 120.632514135532 40
RN1	1.387312209716	302	A_CCN2 121.520257471741 41
RN1_	1.306774234099	303	A_NC1 178.892616155745 42
RCC1	1.396284972460	4	A_NC2 178.572068150837 43
RCC1_	1.452649592801	305	ACO 121.125633135223 335
RCC2	1.390308869238	6	ACH1 119.875843606016 46
RCC2_	1.343435765064	307	ACH1_ 120.468355855165 347
RCC3	1.410222928846	8	ACH2_ 121.910346465997 49
RCC3_	1.478155933854	309	ACH3 119.182724604862 50
RCC4	1.398027850847	10	ACH3_ 116.654847705801 351
RCC4_	1.467522327509	311	ACH4 120.073652928975 352
RCC5	1.400215230760	12	ACH4_ 116.447845645714 353
RCC6	1.380186377628	14	ANH 121.313578584539 345
RCC5_	1.449803573929	313	T 180.000000000000 54
RCC6_	1.343906466347	315	T1 0.000000000000 55
R_CCN1	1.429876167723	16	T1_ 0.000000000000 56
R_CCN2	1.424803149448	17	T2 180.000000000000 57
RNC1	1.150927285399	18	T2_ 180.000000000000 58
RNC2	1.151973935740	19	TPh1 0.000000000000 59
RCO	1.223602404077	320	TPh1_ 0.000000000000 60
RCH1	1.077657064801	22	TPh2 0.000000000000 61
RCH1_	1.082945724892	23	TPh2_ 0.000000000000 62
RCH2_	1.081475582676	25	TPh3 180.000000000000 63
RCH3	1.080030802068	26	TPh3_ 180.000000000000 64
RCH3_	1.080867059541	27	T_CCN1 180.000000000000 65
RCH4	1.082375983319	28	T_CCN2 180.000000000000 66
RCH4_	1.081769810910	29	T_NC1 180.000000000000 67
RNH	1.011860771403	321	T_NC2 0.000000000000 68
AN1	121.348780321068	330	TCO 180.000000000000 69
AN1_	121.303890665765	331	TH1 180.000000000000 71
AC1	121.484778852341	332	TH1_ 180.000000000000 72
AC1_	126.551815674281	333	TH2 180.000000000000 73
AC2	119.803277789354	34	TH2_ 180.000000000000 75
AC2_	120.747875213176	34	TH3 180.000000000000 76
AC3	120.671610605093	34	TH3_ 180.000000000000 77
AC3_	122.055602480512	34	TH4 180.000000000000 77
AC4	118.644659599347	34	TH4_ 179.999998792582 78
AC4_	116.124183562881	34	TNH 0.000000000000 70

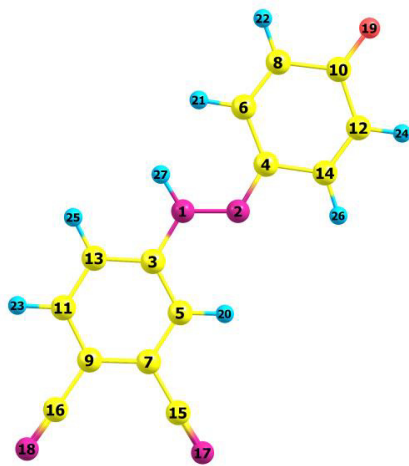


Table S6. Z-matrix was used for model *f* in the GED refinement.

Body of Z-matrix			
1 N			
2 N 1 NN			
3 C 1 RN1 2 AN1			
4 C 2 RN1_1 AN1_3 T			
5 C 3 RCC1 1 AC1 2 T1			
6 C 4 RCC1_2 AC1_1 T1_			
7 C 5 RCC2 3 AC2 1 T2			
8 C 6 RCC2_4 AC2_2 T2_			
9 C 7 RCC3 5 AC3 3 TPh1			
10 C 8 RCC3_6 AC3_4 TPh1_			
11 C 9 RCC4 7 AC4 5 TPh2			
12 C 10 RCC4_8 AC4_6 TPh2_			
13 C 3 RCC5 11 RCC6 5 TPh3 4			
14 C 4 RCC5_12 RCC6_6 TPh3_ 4			
15 C 7 R_CCN1 9 A_CCN1 5 T_CCN1			
16 C 9 R_CCN2 7 A_CCN2 11 T_CCN2			
17 N 15 RNC1 7 A_NC1 9 T_NC1			
18 N 16 RNC2 9 A_NC2 11 T_NC2			
19 O 10 RCO 8 ACO 12 TCO			
20 H 5 RCH1 3 ACH1 7 TH1			
21 H 6 RCH1_4 ACH1_8 TH1_			
22 H 8 RCH2_6 ACH2_10 TH2			
23 H 11 RCH3 9 ACH3 13 TH3			
24 H 12 RCH3_10 ACH3_14 TH3_			
25 H 13 RCH4 3 ACH4 11 TH4			
26 H 14 RCH4_4 ACH4_12 TH4_			
27 H 1 RNH 2 ANH 4 TNH			
Variables Values		Atom numbering	
NN	1.323058830514	301	A_CCN1 121.056390900073 40
RN1	1.387504404705	302	A_CCN2 121.388792727409 41
RN1_	1.307112199019	303	A_NC1 178.530412440200 42
RCC1	1.396282957021	4	A_NC2 178.707243655461 43
RCC1_	1.452572849935	305	ACO 121.167922989125 335
RCC2	1.390373730658	6	ACH1 120.556862012080 446
RCC2_	1.343544417148	307	ACH1_ 120.478894195395 347
RCC3	1.409062479000	8	ACH2_ 121.891667954206 49
RCC3_	1.477978891977	309	ACH3 118.924447187790 50
RCC4	1.399067521505	10	ACH3_ 116.645738137707 351
RCC4_	1.467631925459	311	ACH4 119.452154714838 352
RCC5	1.400204735760	12	ACH4_ 116.447762940886 353
RCC6	1.380529364615	14	ANH 121.270561118437 345
RCC5_	1.449652935218	313	T 180.000000000000 54
RCC6_	1.343893534222	315	T1 180.000000000000 55
R_CCN1	1.429148666963	16	T1_ 0.000000000000 56
R_CCN2	1.424750570000	17	T2 180.000000000000 57
RNC1	1.151040471209	18	T2_ 180.000000000000 58
RNC2	1.151973077854	19	TPh1 0.000000000000 59
RCO	1.223598387917	320	TPh1_ 0.000000000000 60
RCH1	1.081571091008	22	TPh2 0.000000000000 61
RCH1_	1.082909673870	23	TPh2_ 0.000000000000 62
RCH2_	1.081457695706	25	TPh3 180.000000000000 63
RCH3	1.080256335054	26	TPh3_ 180.000000000000 64
RCH3_	1.080881675556	27	T_CCN1 180.000000000000 65
RCH4	1.078042778237	28	T_CCN2 180.000000000000 66
RCH4_	1.081779645141	29	T_NC1 180.000000000000 67
RNH	1.011981327227	321	T_NC2 0.000000000000 68
AN1	121.300828452407	330	TCO 180.000000000000 69
AN1_	121.268513759707	331	TH1 179.999998792582 71
AC1	118.439751194757	432	TH1_ 180.000000000000 72
AC1_	126.579517920234	333	TH2 180.000000000000 73
AC2	120.394566233865	34	TH3 180.000000000000 75
AC2_	120.751418382878	34	TH3_ 180.000000000000 76
AC3	120.121591762435	34	TH4 180.000000000000 77
AC3_	122.061658394255	34	TH4_ 180.000000000000 78
AC4	118.638968567670	34	TNH 0.000000000000 70
AC4_	116.117326024308	34	

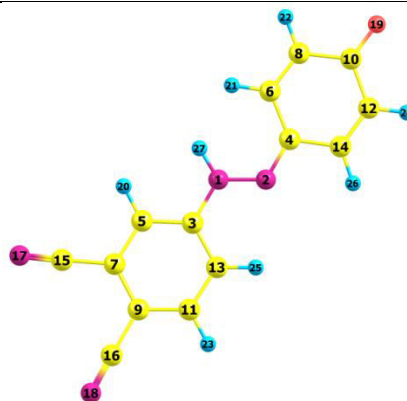


Table S7. Nucleus-independent chemical shifts (NICS)^a indexes for *E-AB* and *p-HPhAPN*

Structure (see Figures 1-2)	<i>E-AB</i>	<i>p-HPhAPN</i>					
		<i>a</i>	<i>e</i>	<i>g</i>	<i>za</i>	<i>ze</i>	<i>zg</i>
		for phenyl moiety substituted by two –CN groups					
NICS(0)	-7.0	-7.8	-8.2	-7.2	-8.6	-8.4	-7.3
NICS(1)	-8.8	-8.7	-8.5	-8.0	-8.8	-8.5	-7.8
		for phenyl moiety substituted by –OH/O group					
NICS(0)'	-7.0	-6.9	3.9	2.5	-8.6	4.9	1.9
NICS(1)'	-8.8	-7.9	-1.0	-1.7	-8.7	-0.4	-1.8

^a For comparison, the corresponding values of the initial compounds were found: Benzene: NICS(0)=-8.1, NICS(1)=-9.9; Phenol: NICS(0)=-9.0, NICS(1)=-9.4; Phthalonitrile: NICS(0)=-8.7, NICS(1)=-9.8.

Table S8. Electron delocalization indexes (DI) calculated by QTAIM for several structures of *p-HPhAPN*.

Structure (see Figures 1-2)	<i>a</i>	<i>e</i>	<i>g</i>	<i>za</i>	<i>ze</i>
DI(N1-N'1)	1.86	1.38	1.48	1.93	1.31
DI(N1-C2)	1.06	1.01	1.12	1.03	1.02
DI(N'1-C'2)	1.08	1.35	1.15	1.04	1.40
DI(O-C)	0.94	1.34	1.33	0.94	1.35
DI(O-C)	1.28	1.08	1.13	1.28	1.07
DI(C2'-C3')	1.26	1.09	1.13	1.29	1.06
DI(C6'-C7')	1.41	1.65	1.61	1.42	1.67
DI(C3'-C4')	1.45	1.66	1.62	1.41	1.67
DI(C5'-C6')	1.30	1.03	1.03	1.27	1.00
DI(C4'-C5')	1.26	1.01	1.03	1.30	1.02

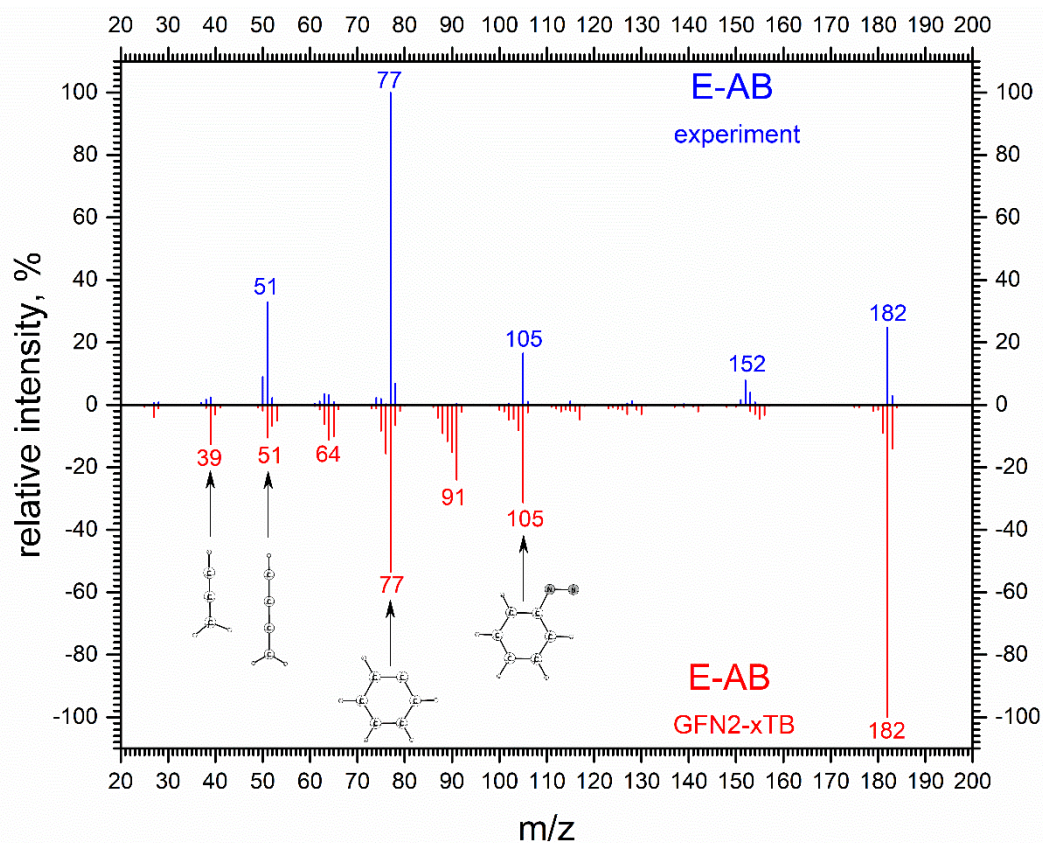


Figure S2. Calculated (GFN2-xTB) EI-MS (below, inverted intensities) of E-AB in comparison with the experimental EI-MS [75] (above).

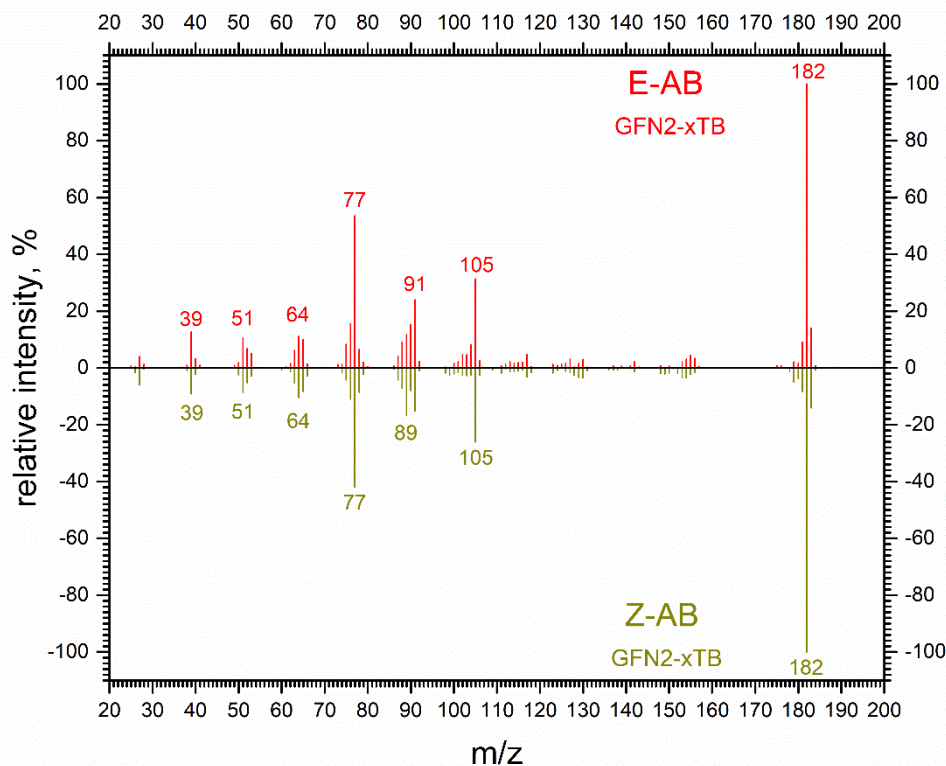


Figure S3. Comparison of EI-MS obtained using the QCxMS (GFN2-xTB) procedures started separately for E-AB (above) and Z-AB (below, inverted intensities) structures.

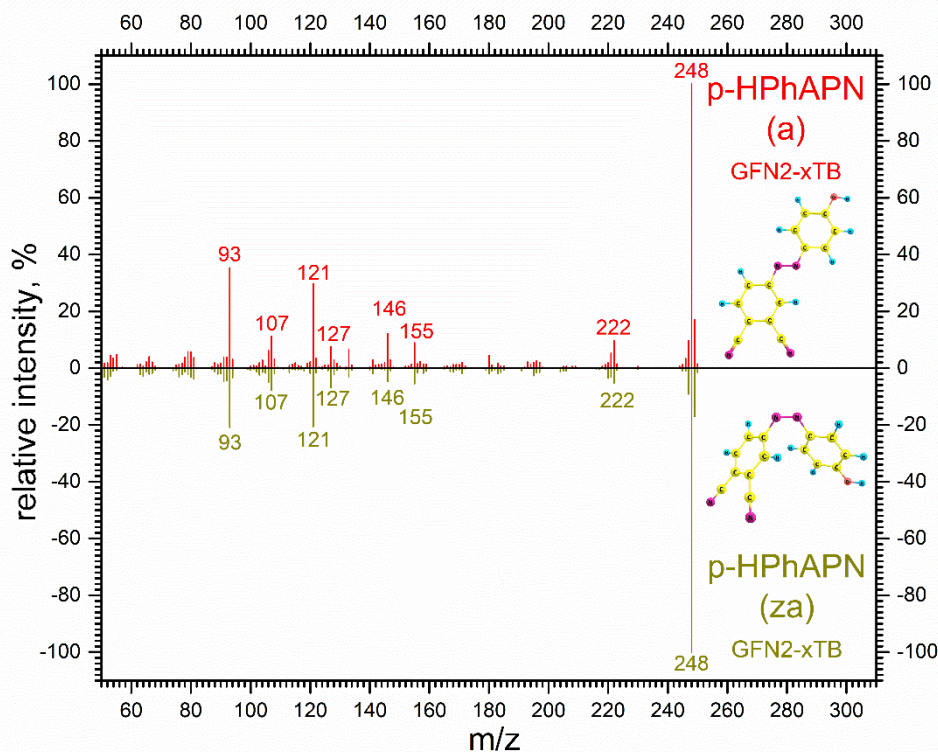


Figure S4. Comparison of EI-MS of *p*-HPhAPN obtained using the QCxMS (GFN2-xTB) procedures started separately for **a** (above) and **za** (below, inverted intensities) structures.

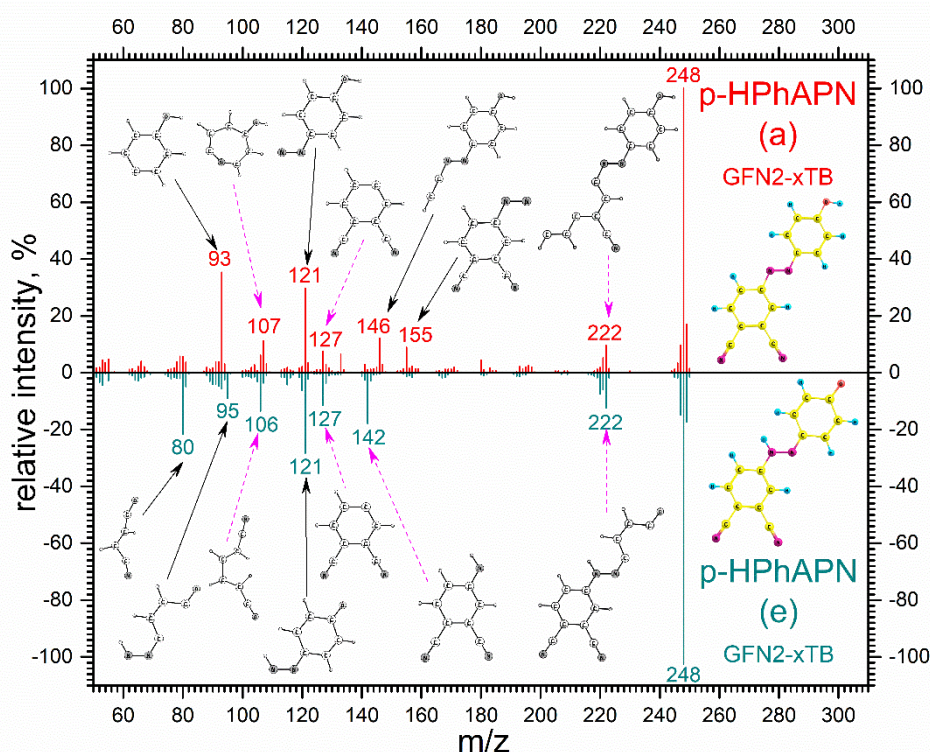


Figure S5. Comparison of calculated (GFN2-xTB) EI-MS of *p*-HPhAPN isomers **a** (above) and **e** (below, inverted intensities).

For assignment black (pink dashed) arrows were used if the contribution of the presented structure to the total intensity is at least (less than) 70%.

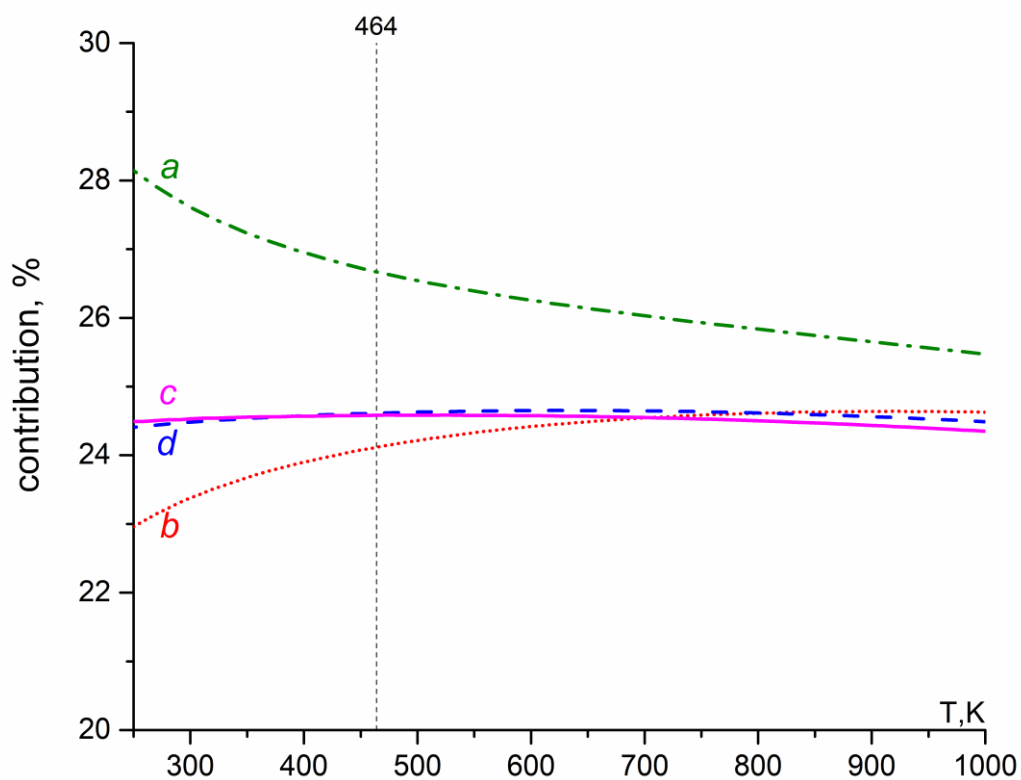


Figure S6. Temperature dependence of conformational/isomeric composition of *p*-HPhAPN. Green dashed and dotted line – conformer **a**, red dotted line – conformer **b**, pink solid line – conformer **c**, blue dashed line – conformer **d**. The dashed vertical line corresponds to the temperature of the GED experiment (464 K). This dependence was calculated using a “rigid rotor - harmonic oscillator” approximation realized in the VibModule program.

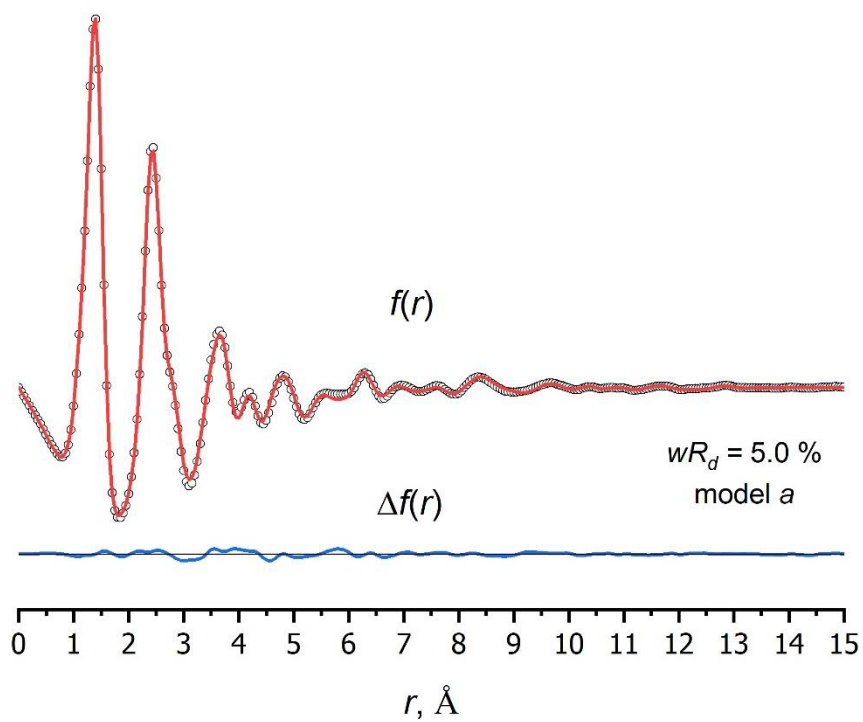
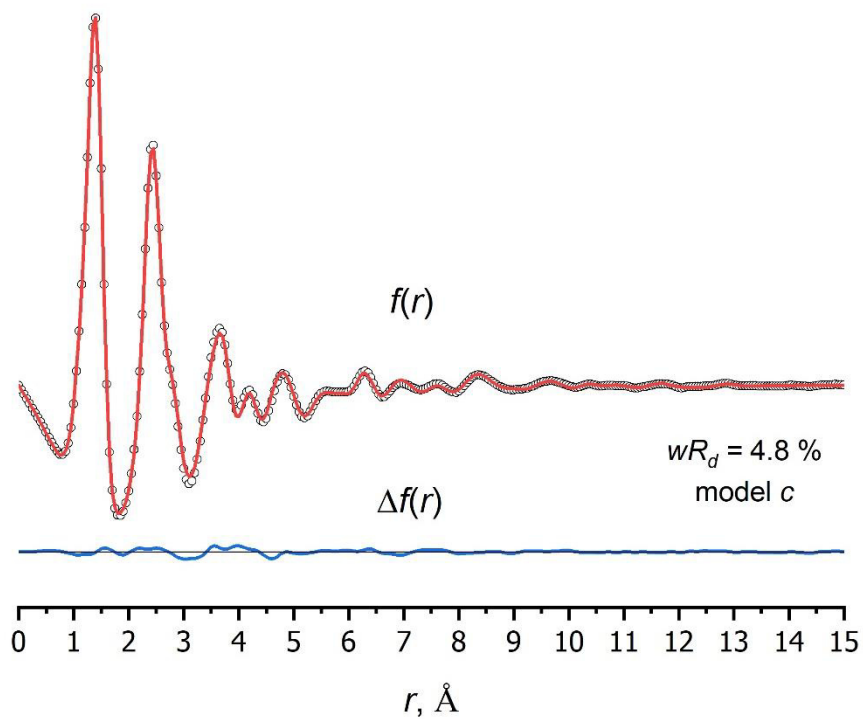


Figure S7. Experimental (cycles) and theoretical (red solid lines) radial distribution curve for models **c** and **a** of **p-HPHAPN** and the difference curve $\Delta f(r)$ (blue solid line).

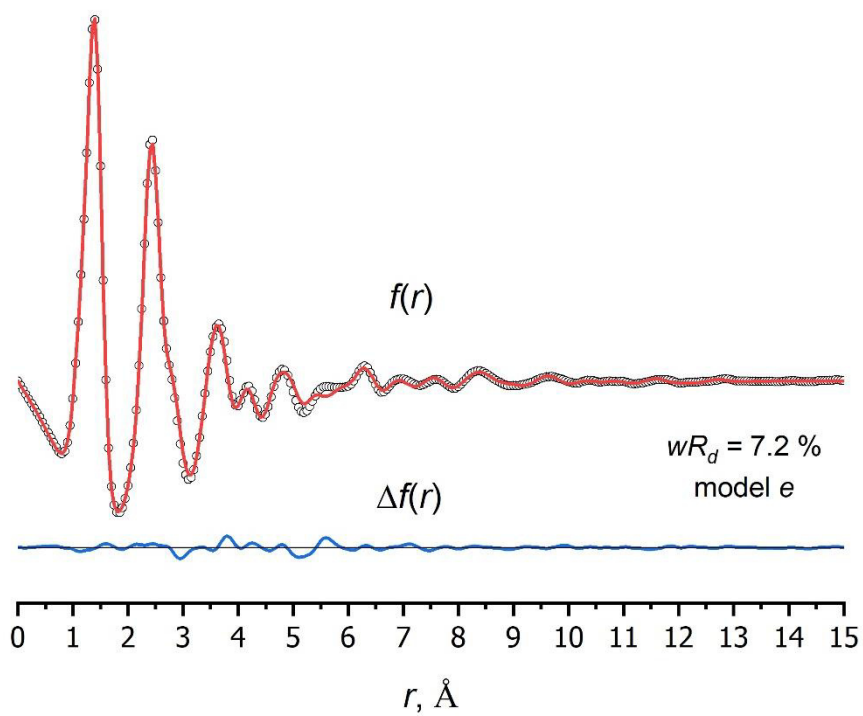
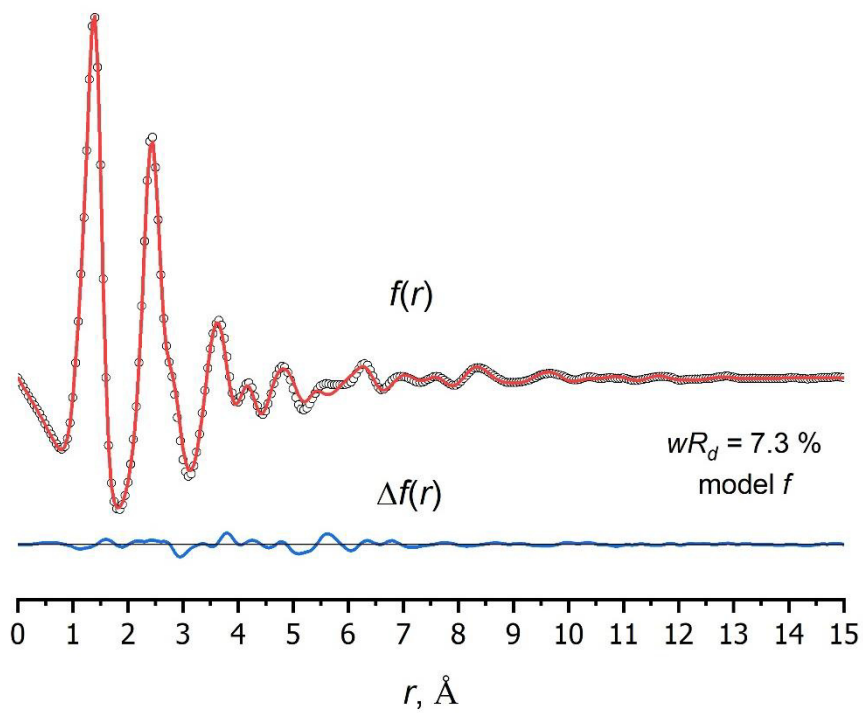


Figure S8. Experimental (cycles) and theoretical (red solid lines) radial distribution curve for models f and e of p -**HPHAPN** and the difference curve $\Delta f(r)$ (blue solid line).

Table S9. Semi-experimental parameters of *p*-HPhAPN (azo forms *a* and *c*).

Atom 1 ^a	Atom 2 ^a	Atom 3 ^a	Atom 4 ^a	<i>a</i>	<i>c</i>
internuclear distances, Å					
1	2			1.250(8)	1.250(8)
1	3			1.415(11)	1.415(11)
2	4			1.396(11)	1.397(11)
3	5			1.393(11)	1.388(11)
3	13			1.401(11)	1.406(11)
4	6			1.402(11)	1.403(11)
4	14			1.398(11)	1.398(11)
5	7			1.385(11)	1.389(11)
5	20			1.081(12)	1.082(12)
6	8			1.365(11)	1.365(11)
6	21			1.082(12)	1.082(12)
7	9			1.427(11)	1.422(11)
7	15			1.434(11)	1.433(11)
8	10			1.393(11)	1.393(11)
8	22			1.083(12)	1.083(12)
9	11			1.399(11)	1.403(11)
9	16			1.432(11)	1.432(11)
10	12			1.392(11)	1.392(11)
10	19			1.331(10)	1.331(10)
11	13			1.384(11)	1.381(11)
11	23			1.083(12)	1.083(12)
12	14			1.377(11)	1.377(11)
12	24			1.085(12)	1.085(12)
13	25			1.083(12)	1.082(12)
14	26			1.083(12)	1.083(12)
15	17			1.155(10)	1.155(10)
16	18			1.156(10)	1.156(10)
19	27			0.961(12)	0.961(12)
bond angles, °					
2	1	3		114.9(12)	114.9(12)
1	2	4		116.3(11)	116.1(11)
1	3	5		124.1(13)	115.2(13)
1	3	13		117.3(18)	126.2(18)
2	4	6		125.4(10)	125.3(10)
2	4	14		116.1(17)	116.2(17)
5	3	13		118.5(13)	118.6(13)
3	5	7		120.3(3)	120.9(3)
3	5	20		119.5(14)	118.9(14)
3	13	11		122.8(20)	122.2(20)
3	13	25		118.5(14)	119.1(14)
6	4	14		118.5(13)	118.5(13)
4	6	8		120.4(3)	120.4(3)
4	6	21		119.1(14)	119.1(14)
4	14	12		121.5(22)	121.5(22)

4	14	26		118.5(14)	118.5(14)
7	5	20		120.2(14)	120.2(14)
5	7	9		120.4(3)	119.9(3)
5	7	15		117.1(12)	117.3(12)
8	6	21		120.4(14)	120.4(14)
6	8	10		120.2(3)	120.3(3)
6	8	22		121.4(14)	121.4(14)
9	7	15		122.6(12)	122.9(12)
7	9	11		119.5(3)	119.5(3)
7	9	16		122.9(12)	123.0(12)
7	15	17		178.3(13)	178.3(13)
10	8	22		118.3(14)	118.3(14)
8	10	12		120.6(3)	120.5(3)
8	10	19		116.7(13)	116.7(13)
11	9	16		117.6(13)	117.5(13)
9	11	13		118.5(14)	119.0(14)
9	11	23		119.2(14)	118.9(14)
9	16	18		178.3(14)	178.2(14)
12	10	19		122.8(14)	122.8(14)
10	12	14		118.7(16)	118.7(16)
10	12	24		120.1(14)	120.1(14)
10	19	27		110.5(14)	110.5(14)
13	11	23		122.3(20)	122.1(20)
11	13	25		118.7(24)	118.7(24)
14	12	24		121.2(21)	121.2(21)
12	14	26		120.0(26)	119.9(26)
dihedral angles, °					
4	2	1	3	-180.0(14)	-180.0(14)
2	1	3	5	0.0(14)	180.0(14)
2	1	3	13	180.0(25)	0.0(27)
1	2	4	6	0.0(14)	0.0(14)
1	2	4	14	-180.0(25)	-180.0(25)
1	3	5	7	180.0(14)	180.0(14)
1	3	5	20	0.0(19)	0.0(19)
1	3	13	11	-180.0(21)	-180.0(24)
1	3	13	25	0.0(25)	0.0(27)
2	4	6	8	180.0(14)	180.0(14)
2	4	6	21	0.0(19)	0.0(19)
2	4	14	12	-180.0(20)	180.0(20)
2	4	14	26	0.0(24)	0.0(24)
7	5	3	13	0.0(17)	0.0(17)
20	5	3	13	-180.0(22)	-180.0(22)
5	3	13	11	0.0(15)	0.0(15)
5	3	13	25	-180.0(21)	-180.0(21)
3	5	7	9	0.0(14)	0.0(14)
3	5	7	15	180.0(19)	180.0(19)
3	13	11	9	0.0(24)	0.0(24)
3	13	11	23	180.0(28)	180.0(28)

8	6	4	14	0.0(17)	0.0(17)
21	6	4	14	180.0(22)	180.0(22)
6	4	14	12	0.0(15)	0.0(15)
6	4	14	26	-180.0(21)	180.0(21)
4	6	8	10	0.0(14)	0.0(14)
4	6	8	22	-180.0(19)	-180.0(19)
4	14	12	10	0.0(24)	0.0(24)
4	14	12	24	180.0(28)	-180.0(28)
9	7	5	20	180.0(19)	180.0(19)
15	7	5	20	0.0(23)	0.0(23)
5	7	9	11	0.0(14)	0.0(14)
5	7	9	16	-180.0(19)	-180.0(19)
5	7	15	17	0.0(19)	0.0(19)
10	8	6	21	-180.0(19)	-180.0(19)
22	8	6	21	0.0(24)	0.0(24)
6	8	10	12	0.0(14)	0.0(14)
6	8	10	19	-180.0(19)	-180.0(19)
11	9	7	15	180.0(19)	180.0(19)
16	9	7	15	0.0(24)	0.0(24)
9	7	15	17	180.0(14)	180.0(14)
7	9	11	13	0.0(25)	0.0(25)
7	9	11	23	-180.0(28)	-180.0(29)
7	9	16	18	180.0(19)	180.0(19)
12	10	8	22	-180.0(19)	-180.0(19)
19	10	8	22	0.0(23)	0.0(23)
8	10	12	14	0.0(25)	0.0(25)
8	10	12	24	-180.0(29)	180.0(29)
8	10	19	27	-180.0(19)	180.0(19)
13	11	9	16	-180.0(28)	-180.0(28)
23	11	9	16	0.0(31)	0.0(31)
11	9	16	18	0.0(14)	0.0(14)
9	11	13	25	180.0(28)	180.0(28)
14	12	10	19	-180.0(29)	180.0(29)
24	12	10	19	0.0(32)	0.0(32)
12	10	19	27	0.0(14)	0.0(14)
10	12	14	26	180.0(28)	-180.0(28)
25	13	11	23	0.0(31)	0.0(31)
26	14	12	24	0.0(31)	0.0(31)
20	5	3	7	0.0(12)	0.0(12)
25	13	3	11	0.0(12)	0.0(12)
21	6	4	8	0.0(12)	0.0(12)
26	14	4	12	0.0(12)	0.0(12)
22	8	6	10	0.0(12)	0.0(12)
23	11	9	13	0.0(12)	0.0(12)
24	12	10	14	0.0(12)	0.0(12)

^a Numbering from Tables S3-S4;

^b uncertainties for the bond lengths were estimated as $[(2.5\sigma_{LS})^2 + (0.002r)^2]^{1/2}$; uncertainty for the angle was estimated as $3\sigma_{LS}$.

Table S10. Relative energies^a of different isomers of **Zn-tHPhDaPc** obtained using different forms (**a**, **c**, **e**, **f**) of **p-HPhAPN**.

Isomer	Form of of p-HPhAPN	Relative energy, kJ·mol ⁻¹
I	a	4.1
II	a	5.3
III	a	4.9
IV	a	4.7
I	c	0.0
II	c	0.0
III	c	0.2
IV	c	0.0
I	e	104.6
II	e	105.7
III	e	105.2
IV	e	105.2
I	f	102.4
II	f	104.5
III	f	103.5
IV	f	103.3

^a according to B3LYP-D3/pcseg-2 calculations

Table S11. Internuclear distances (Å)^a of zinc complex **Zn-tHPhDaPc** obtained using **a** and **c** forms of **p-HPhAPN** and corresponding Internuclear distances of **p-HPhAPN** (models **a** and **c**).

	Zn-tHPhDaPc (I)		p-HPhAPN	
	C_{4v}		C_s	
	a	c	a	c
N-N	1.251	1.251	1.252	1.252
N-C	1.406	1.406	1.400	1.400
N-C	1.413	1.412	1.414	1.414
C _δ -C _δ	1.408	1.413	1.396	1.401
C _γ -C _δ	1.386	1.382	1.384	1.380
C _γ -C _δ	1.400	1.395	1.398	1.393
C _γ -C _β	1.390	1.394	1.396	1.400
C _γ -C _β	1.382	1.386	1.389	1.393
C _β -C _β	1.410	1.406	1.413	1.409

^a according to B3LYP-D3/pcseg-2 calculations

Table S12. Nucleus-independent chemical shifts (NICS)^a indexes for Zinc phthalocyanine (**ZnPc**) and **Zn-tHPhDaPc**.

Structure	ZnPc	Zn-tHPhDaPc	
		I a	I c
for phenyl moiety of phtalocyanine core			
NICS(0)	-7.5	-6.5	-6.0
NICS(1)	-9.4	-8.3	-8.0
for phenyl moiety of azo substituent			
NICS(0) '	-	-7.0	-7.1
NICS(1) '	-	-7.8	-7.9

^a For comparison, the corresponding values of the initial compounds were found: Benzene: NICS(0)=-8.1, NICS(1)=-9.9; Phenol: NICS(0)=-9.0, NICS(1)=-9.4; Phthalonitrile: NICS(0)=-8.7, NICS(1)=-9.8.

[75] NIST Mass Spectrometry Data Center, William E. Wallace, director, "Mass Spectra" in NIST Chemistry WebBook, NIST Standard Reference Database Number 69, Eds. P.J. Linstrom and W.G. Mallard, National Institute of Standards and Technology, Gaithersburg MD, 20899, <https://doi.org/10.18434/T4D303>